THE UNIVERSITY *of* EDINBURGH

Quantum Limited Optical Receivers in the Presence of Intersymbol Interference

Citation for published version:
Huang, S & Safari, M 2020, 'Quantum Limited Optical Receivers in the Presence of Intersymbol Interference', Paper presented at The 45th European Conference on Optical Communication, 22/09/19 - 26/09/19. https://doi.org/10.1049/cp.2019.1129

Digital Object Identifier (DOI):
10.1049/cp.2019.1129

Quantum Limited Optical Receivers in the Presence of Intersymbol Interference

Shenjie Huang[1] , Majid Safari[1]*

[1]*Institute for Digital Communications, School of Engineering, University of Edinburgh, Edinburgh, UK*
**E-mail: shenjie.huang@ed.ac.uk*

Keywords: intersymbol interference (ISI), single-photon avalanche diode (SPAD), dead time

Abstract

The ISI effect due to the dead time of practical photon counting receivers is studied. Using both the counts and arrival times of photons, a novel demodulation technique is proposed showing sensitivity levels around 7 dB beyond traditional photon counting schemes.

1 Introduction

In recent decades, there has been a growing interest of employing photon counting detectors in both fiber [1] and optical wireless communication (OWC) systems [2, 3] to improve the sensitivity of receivers. To realize a photon counting receiver, the commonly used avalanche photodiode (APD) can be biased above the breakdown voltage so that it operates at Geiger mode. By doing so, a single-photon counting avalanche diode (SPAD) can be achieved which has the advantages of single photon sensitivity and picosecond temporal resolution. Large arrays of SPADs that can be employed for imaging and high-speed communication applications are now commercially available. In [1], the experimental results of a SPAD-based optical fiber receiver are presented and a measurement of -55.7 dBm and -51.6 dBm sensitivities at a data rate of 50 Mbit/s and 100 Mbit/s for a BER of 2×10^{-3} is achieved. However, the corresponding quantum limits are -73 dBm and -70 dBm, respectively. Therefore, the sensitivities of the currently available SPAD receivers are still far away from the quantum limit. This is mainly due to the non-ideality effects of SPADs such as their *dead time* when they become inactive for a period of several nanoseconds. The dead time typically happens following the avalanche caused by each photon detection when the SPAD is getting quenched. There are two types of quenching circuits in SPAD receivers, i.e., active quenching (AQ) and passive quenching (PQ). The dead time of AQ SPADs is constant, whereas for PQ SPADs the photons arriving during the dead time can extend its duration [4].

In the literature, the performance degradation of SPAD-based communication systems introduced by dead time is not well investigated. Some studies assume that the received photon count is an ideal Poisson distributed random variable (RV) with the incident photon rate as its mean. However, this model completely ignores the dead time effect and as a result the BER performance is significantly overestimated as shown in [3]. Some other works employ the effects of dead time by assuming that the detected photon count is Poisson random variable with an effective average rate defined based on the dead time [5, 6]. There are two issues regarding this assumption. Firstly, these effective rates are only valid when the symbol duration is much longer than dead time. For high speed data transmission where the symbol time is comparable or even less than the dead time, such approximation is not valid [7]. Secondly, by using this assumption the intersymbol interference (ISI) caused by dead time is ignored. In practical high speed SPAD-based systems, the effect of dead time is more crucial particularly when the dead time started in a symbol extends to the next symbol causing an ISI effect that cannot be ignored.

In [7], the accurate probability mass functions (PMFs) of the detected photon counts for both PQ and AQ SPADs have been derived; however, in this work the ISI effect is also ignored by assuming that the SPAD is always active at the beginning of each symbol duration to simplify the mathematical derivations. Some equalization methods originally designed for RF systems with linear channel expressions have been applied to SPAD-based OWC systems [8]. However, SPAD-based channels require novel demodulation techniques to reduce the impacts of ISI based on the special characteristics of SPADs, which is still a research gap in the literature to the best of authors' knowledge. In this paper, an effective demodulation technique for SPAD-based communication systems using the photon arrival time information is proposed to remarkably improve the BER performance.

2 Photon Counting in the Presence of ISI

2.1 the Effects of ISI

Since SPAD is extremely sensitive to photon arrivals, when a photon triggers an avalanche event, an electrical pulse signal at the output of SPAD can be detected. However, due to the existence of dead time, the SPAD remains blind to the incident photons for a short time τ_d after a photon is detected. Note that in this work, we focus on AQ SPADs for its simplicity in dead time behaviour. An example of the detected photon arrival sequence is plotted in Fig. 1. In this figure, we denote the start and the end of the considered symbol period as $T_{\rm st}$ and $T_{\rm st} + T_s$, respectively, where T_s refers to the symbol duration. In the

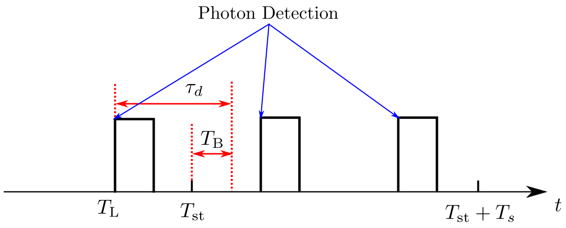

Fig. 1: The photon arrival sequence.

presence of ISI, the SPAD might be inactive at the beginning of the counting duration until the end of the dead time introduced by the last photon arrived in the previous symbol. We denote this inactive period at the beginning of the current counting period as the *block time* T_{B} which can be expressed as

$$T_{\mathrm{B}} = \max\left\{\tau_d - \left(T_{\mathrm{st}} - T_{\mathrm{L}}\right), 0\right\}, \tag{1}$$

where T_{L} is the last photon arrival time before the start of the counting period. In the presence of ISI, the SPAD is actually only active from $T_{\mathrm{st}} + T_{\mathrm{B}}$ rather than T_{st} in the absence of ISI. Since T_{L} is itself a RV, the ISI introduces a random inactive time which changes the statistics of the photon count during the considered symbol duration. In practical systems, SPAD array is commonly employed to improve the dynamic range of the receiver and control the saturation issue of such sensitive receivers. Similar to the case of single SPAD, ISI also influences the statistics of the total photon counts in an array. In Fig. 2, the effect of ISI can be observed by comparing the conditional PMFs of the received photon count in the presence and the absence of of ISI when NRZ OOK signals are transmitted. One can observe that with relatively small dead time, e.g., $\tau_d = 0.5T_s$, the PMFs of photon count in the presence of ISI deviate slightly from those in the absence of ISI. However, for a relatively large dead time, e.g., $\tau_d = T_s$, a significant mismatch between them are observed. This mismatch of PMFs is due to the fact that for longer dead time, the probability that the number of SPADs being inactive at the beginning of the current symbol increases. As a result, the ISI effect becomes more severe and the probability of detecting less photon counts increases. It is also demonstrated in Fig. 2 that ISI results in smaller average value and larger variance of the detected photon count. These effects of ISI on the statistics of the detected photon count can significantly increase error probability in the communication systems.

The ISI effects are not only related to the dead time but also related to the incident photon rate (both signal and background photon rates). SPAD array with larger number of SPADs is commonly employed to mitigate the ISI effects by means of diversity [3]; however, ISI effects could still be significant especially when the incident photon rate is high and/or the SPAD array is employed in high-speed systems where dead time is comparable or even longer than the symbol time. It is worth emphasizing that the effects of ISI in SPAD-based system is different from that in traditional communication systems. In traditional systems, the effect of channels can be described as a lowpass filter so that various equalizers (either linear or nonlinear) can be employed to compensate the lowpass effects.

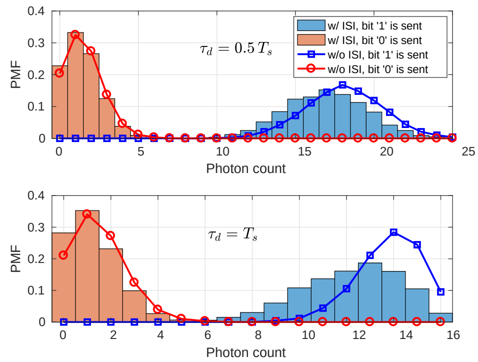

Fig. 2: The conditional PMF of the detected photon count for a SPAD array with $N = 16$ in the presence and absence of ISI. OOK signal is transmitted. The photon rates (for each individual SPAD) for bit '1' and bit '0' transmission are 2 and 0.1, respectively.

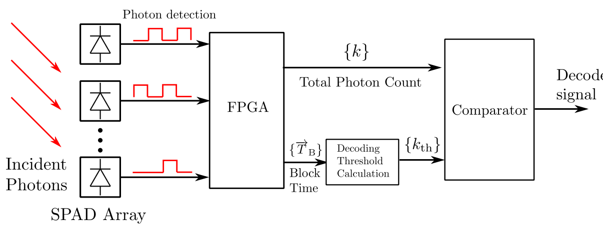

Fig. 3: The schematic of the proposed demodulation technique.

However, this is not the case in SPAD based channel, since by introducing the random block time T_{B} ISI acts as an additional source of random noise and the channel itself cannot be expressed as a lowpass form. As a result, the commonly used equalizers designed for lowpass channels cannot achieve optimal performance in SPAD-based systems.

2.2 *Proposed Demodulation Scheme*

SPADs can provide both photon counts and accurate photon arrival times [9, 10]. Inspired by this capability, in this work we propose a new demodulation technique using both photon counts and their arrival times. We consider OOK modulation as an example, although the proposed idea can also be applied to systems with other modulation schemes.

The schematic of the proposed scheme is plotted in Fig. 3. The photon arrival sequences of the SPAD array are sent to the FPGA for extracting the total photon count and photon arrival time information. Using the photon arrival time information, the block time can be calculated based on (1). Note that for the array-based receiver, the block times of SPAD elements are different from each other and hence a block time vector $\vec{T}_{\mathrm{B}}$ is required to be calculated. The block time information is then used to calculate the decision threshold k_{th} and the signal is demodulated by comparing the photon count with k_{th}. Different from the traditional system in the literature in which the decoding threshold is fixed, in our system the threshold is calculated using the instantaneous block time information and hence is adapted to the instantaneous ISI status. It is expected that the degradation introduced by ISI effects can be minimized using such adaptive decision threshold.

3 Error Performance Analysis

For high-speed optical communication systems, in order to achieve higher data rates, it is very likely that the links are operated in sub-dead-time regimes where the symbol duration is equal or less than the dead time. In such sub-dead-time regime, a SPAD can at most detect one photon in a symbol duration. Therefore, the photon counting process becomes a Bernoulli process. For the array-based receiver, in the absence of ISI, the total photon count can be modeled as a Binomial distributed RV because of the identical probability of detecting a photon in every SPAD [11]. However, this is not the case in the presence of ISI, since each SPAD has different probability of detecting a photon. For the nth SPAD in the array, the PMF of the photon count is given by

$$p_k(k; T_{\mathrm{B},n}, \lambda) = \begin{cases} \exp\left[-\lambda\left(T_s - T_{\mathrm{B},n}\right)\right], & k = 0, \\ 1 - \exp\left[-\lambda\left(T_c - T_{\mathrm{B},n}\right)\right], & k = 1, \end{cases} \quad (2)$$

where λ refers to the average detected photon rate. Thus, the total photon counts of SPAD array are the sum of Bernoulli RVs with different probabilities of success which are determined by the block time vector $\overrightarrow{T}_{\mathrm{B}} = \{T_{\mathrm{B},1}, T_{\mathrm{B},2}, \cdots, T_{\mathrm{B},N}\}$. The total photon count K hence should follow the Poisson Binomial distribution with PMF

$$p_K(K; \overrightarrow{T}_{\mathrm{B}}, \lambda) = \quad (3)$$
$$\sum_{\vartheta \in F_K} \prod_{i \in \vartheta} 1 - \exp[-\lambda\left(T_c - T_{\mathrm{B},i}\right)] \prod_{j \in \vartheta^c} \exp\left[-\lambda\left(T_c - T_{\mathrm{B},j}\right)\right],$$

where F_k is the set of all subsets of K integers that can be chosen from $\{1, 2, \cdots, N\}$, N denotes the number of SPADs in the array, and ϑ^c is the complement of the subset ϑ. Considering the ML decoding, the optimal decision threshold K_{th} conditioned on $\overrightarrow{T}_{\mathrm{B}}$ is given by the crosspoint of $p_K(K; \overrightarrow{T}_{\mathrm{B}}, \lambda_0)$ and $p_K(K; \overrightarrow{T}_{\mathrm{B}}, \lambda_1)$ where λ_0 and λ_1 denote the detected photon rate per SPAD when bit '0' and bit '1' are sent, respectively. This threshold can be calculated numerically.

We present some simulation results to show the advantage of our proposed demodulation scheme over state of the art. Four systems are considered in the simulation study. The first system refers to the ideal system considering dead time but ignoring the ISI effect. The second system is impaired by ISI but the demodulator ignores the ISI effect. Such system represents the practical SPAD-based system without addressing ISI. In the third system (denoted as the system with ES), a fixed decision threshold which minimizes the BER over all symbols is determined based on an exhaustive search by using the histogram of the received photon count. The fourth system refers to the one employs the proposed demodulation technique as shown in Fig. 3. An array of 8 SPADs is assumed, the dead time τ_d is considered as 10 ns, the diameter of active area of each SPAD is 30 μm, the photon detection probability is 27% and the wavelength of the signal light is 650 nm. Figure 4 shows the BER performance of the considered four systems with respect to the average detected signal photon rate per SPAD. It is clear that under weak background photon rate $\lambda_0 = 1$ kHz, the system

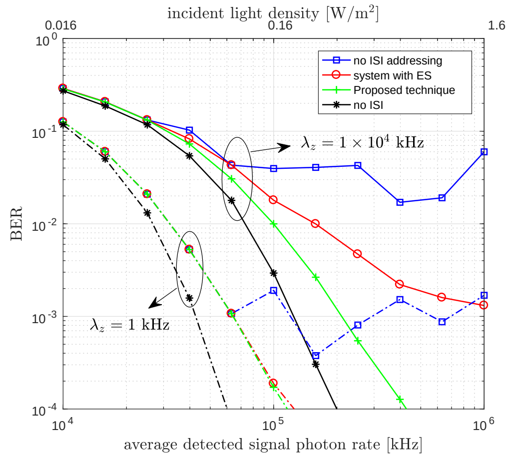

Fig. 4: The BER versus the average detected signal photon rate per SPAD (bottom x-axis) and corresponding incident light intensity (top x-axis) for the considered systems under various background photon rate where $N = 8$ and the dead time to symbol duration ratio is 1.1.

operates in the absence of ISI outperforms the other three in the presence of ISI, which reveals that the degradation caused by ISI is non-negligible even under such weak background light intensity. Also, it is shown that the system with ES is similar to that with the proposed technique and both perform significantly better than that without addressing ISI. Note that the performance curve of the system without addressing ISI is not smooth due to the blindness of the system to the ISI. When significant background light is considered, e.g., $\lambda_0 = 10^4$ kHz (light density 16 mW/m^2), ISI effects become more severe and the performance of all systems are degraded. The advantages of the system with the proposed technique (green solid curve) over the system with ES (red solid curve) become obvious now. One can see that under such background light intensity, for the system with proposed scheme, an average signal photon rate of 1.95×10^5 kHz (1.75 photons/bit/ SPAD) is required to achieve a BER of 1.3×10^{-3}; whereas for the system with ES, the corresponding required signal photon rate increase to 10^6 kHz (9 photons/bit/ SPAD). Hence a 7.1 dB increase of receiver sensitivity can be achieved by using the proposed scheme. In addition, with the increase of the signal photon rate, higher sensitivities are expected to be achieved.

4 Conclusion

A novel demodulation technique for photon counting communication systems is designed. The photon arrival information is incorporated in the decoding process. It is demonstrated that by using the proposed scheme, significant BER improvement can be observed. The proposed scheme has the potential to enhance the tolerance of the SPAD-based systems to the background light.

5 Acknowledgements

The authors gratefully acknowledge the financial support from EPSRC under grant EP/R023123/1 (ARROW).

6 References

[1] H. Zimmermann, B. Steindl, M. Hofbauer, and R. Enne, "Integrated fiber optical receiver reducing the gap to the quantum limit," *Scientific reports*, vol. 7, no. 1, p. 2652, 2017.

[2] E. Fisher, I. Underwood, and R. Henderson, "A reconfigurable single-photon-counting integrating receiver for optical communications," *IEEE Journal of Solid-State Circuits*, vol. 48, no. 7, pp. 1638–1650, July 2013.

[3] D. Chitnis and S. Collins, "A spad-based photon detecting system for optical communications," *J. Lightwave Technol.*, vol. 32, no. 10, pp. 2028–2034, May 2014.

[4] S. Cova, M. Ghioni, A. Lacaita, C. Samori, and F. Zappa, "Avalanche photodiodes and quenching circuits for single-photon detection," *Appl. Opt.*, vol. 35, no. 12, pp. 1956–1976, Apr 1996.

[5] Y. Li, M. Safari, R. Henderson, and H. Haas, "Nonlinear distortion in spad-based optical ofdm systems," in *2015 IEEE Globecom Workshops (GC Wkshps)*, Dec 2015, pp. 1–6.

[6] ——, "Optical ofdm with single-photon avalanche diode," *IEEE Photonics Technology Letters*, vol. 27, no. 9, pp. 943–946, May 2015.

[7] E. Sarbazi, M. Safari, and H. Haas, "Statistical modeling of single-photon avalanche diode receivers for optical wireless communications," *IEEE Transactions on Communications*, vol. 66, no. 9, pp. 4043–4058, Sep. 2018.

[8] L. Zhang, D. Chitnis, H. Chun, S. Rajbhandari, G. Faulkner, D. O'Brien, and S. Collins, "A comparison of apd- and spad-based receivers for visible light communications," *J. Lightwave Technol.*, vol. 36, no. 12, pp. 2435–2442, Jun 2018.

[9] T. Al Abbas, N. A. W. Dutton, O. Almer, N. Finlayson, F. M. D. Rocca, and R. Henderson, "A cmos spad sensor with a multi-event folded flash time-to-digital converter for ultra-fast optical transient capture," *IEEE Sensors Journal*, vol. 18, no. 8, pp. 3163–3173, April 2018.

[10] A. Griffiths, J. Herrnsdorf, C. Lowe, M. Macdonald, R. Henderson, M. Strain, and M. Dawson, "Temporal encoding to reject background signals in a low complexity, photon counting communication link," *Materials*, vol. 11, no. 9, p. 1671, 2018.

[11] H. Mahmoudi, M. Hofbauer, B. Steindl, K. Schneider-Hornstein, and H. Zimmermann, "Modeling and analysis of ber performance in a spad-based integrated fiber optical receiver," *IEEE Photonics Journal*, vol. 10, no. 6, pp. 1–11, Dec 2018.